Computer Automated Detection of Head Orientation for Prevention of Wrong-Side Treatment Errors

James D. Christensen, PhD [1,2], Gary C. Hutchins, PhD [2], Clement J. McDonald, MD [1]
[1]Regenstrief Institute, Inc. and [2]Department of Radiology,
Indiana University School of Medicine, Indianapolis, IN

Abstract

A medical error can occur when a patient is positioned in a medical imaging device such as an MRI scanner if information regarding their orientation is improperly entered into the device control software .If such an error is not detected and corrected, the erroneous orientation data will be stored in the image header information and will propagate with the images throughout the medical enterprise. Presented here is a fully automated algorithm for computing patient head orientation from the image data and detecting errors in image orientation labeling. This will enable errors in orientation labeling to be corrected at their source when they occur, thus preventing later medical treatment errors related to laterality.

Introduction

Human error is inevitable and is the source of most medical errors. Wrong-side (left versus right) treatment happens infrequently, but when it does the repercussions can be serious and costly for the patient, the medical staff and the hospital where it occurs (1). When errors of laterality affect treatment of the head, it can be quite serious given the sensitivity of the brain and the invasiveness required to gain entry to it. Serious examples of wrong-side treatment have occurred in neurosurgery, head and neck surgery and radiation treatment. Historically, such errors have been rarely documented in the literature outside of lawsuits, but this is changing due to attempts by hospitals, insurers and governments to better identify the incidence and causes of medical errors so that they can be prevented (2-7).

The standard operating procedures in many medical centers have been changed to reduce surgical errors. Human errors resulting from the fast-paced and stressful environment of surgery departments have been addressed by attempting to change the working environment of the medical team. Simple misreading of radiological images can and does occur and has lead to wrong-side treatment (2,3). Such errors can be minimized by changing the medical team procedures for reading images prior to treatment to ensure that left-right sidedness is properly identified. Non-physician staff have been encouraged and empowered to raise questions, and standard procedures now include time-outs immediately prior to surgery and marking and rechecking the proper location for surgery site by multiple persons.

Despite these changes in the treatment environment, wrong-side treatment still can occur when radiological images are mislabeled with respect to left and right sides prior to their inspection by medical staff. A report of the American Academy of Orthopaedic Surgeons states that one factor contributing to wrong side surgery is the following: "The prone or lateral positioning of the patient and incorrectly marked x-rays may be disorienting factors." (5). This can occur, for example, when a radiology technologist fails to select the correct choice for patient orientation when initially entering a patient's data on the imaging modality's computer. A patient's data is usually entered prior to positioning them for the scan. It is possible that the patient's position needs to be changed for the sake of the patient's comfort, to enable an obese person to enter a gantry or for other reasons. After returning to the imaging device's control panel, if the technologist does not change the patient orientation, the acquired images will be automatically mislabeled with respect to left versus right.

Two cases have been documented where CT mislabeling errors resulted in wrong-side surgery on the head (8). CT scans of the paranasal sinuses are normally done with the patient lying prone and entering the CT scanner head first. Occasionally, a patient cannot tolerate this position and is switched to the supine position. In the first case (8), the software toggle indicating patient orientation was not changed to supine, causing the scanner's computer to automatically display the images with left and right sides of the head annotated incorrectly. In the second case (8), orientation mislabeling resulted in the display of the head images incorrectly with respect to the laterality conventions (radiological convention dictates that left side anatomy be displayed on the right side of the image and vice versa). Both of these cases led to wrong-side surgeries, one of which

resulted in a malpractice lawsuit. The same authors estimated that such labeling errors occurred at their large urban hospital at least once per month; these were corrected by radiology personnel, however they caution that the number of undetected errors was unknown (8).

The fact that such errors can occur due to the simple action or inaction of pressing the correct button at the proper time suggests that they could and probably do occur, at least occasionally, at many medical centers. Such labeling errors will be maintained in the PACS image record system and will propagate over the hospital network through the chain of medical care.

By their nature, modern radiological imaging devices such as CT and MRI acquire digital data that are stored on at least moderately high-speed computers. From an informatics viewpoint, this provides an opportunity to bring computer technology to bear on the problem described above at its source, while the images still reside on the scanner and before labeling errors are stored with the images. If computer software could by some means automatically detect a patient's head orientation by analyzing brain images as they are acquired, it could detect any discordance between the selected and measured orientation. The device operator could then be aided by presenting a pop-up message warning of the detected discrepancy and asking for verification of the orientation. This approach follows a principle recommended by The Institute for Healthcare Improvement for reducing medical errors: "Reduce reliance on memory by designing processes with automatic prompts and less reliance on fallible processes." (6,7).

The human brain has inherent left versus right asymmetry that can be detected automatically (9), however required computation times are too long for the clinical application described above. Presented here is a fast and robust method for automatically detecting head orientation on 3D brain images. Straightforward computations on the images provide metrics that are unambiguous indicators of orientation for objects shaped like the human head, which have inherent imbalances in mass distribution.

Methods

Study Population: A total of 202 subjects were studied. 113 subjects were normal healthy people ranging in age from 6 to 65 years. Male and females were approximately equally represented. Half of the normal group (n=56) were randomly chosen and analyzed to determine head shape parameters that

were used to build a prediction equation; this was designated as the Sample Group. The prediction equation was then applied to the remaining normal subjects (n=57) as well as a group of patients (n=89) with psychiatric disorders including schizophrenia (n=65), major depression (n=2) and disruptive behavioral disorder/ADHD (n=22). This group (n=146) was designated the Test Group.

Image Acquisition: MR images of the brain were acquired on two different 1.5T MRI scanners. In each case, three-dimensional T1-weighted images were acquired using a fast steady-state pulse sequence for data acquisition. Images were transferred to a PC workstation for analysis. MRI was used as the image source for this study, although any neuroimaging modality such as CT or PET also could be used. After the first simple thresholding step, the algorithm is identical for any modality. All images were acquired as fully 3D images without gaps, although this is not a strict requirement of the algorithm.

Image Analysis: All analyses were implemented using the Interactive Data Language (Research Systems, Inc.). Total processing time was 2 minutes per subject using a 1.5 GHz Pentium workstation.

Head Segmentation: A threshold was applied to each image to form a binary mask, which has a value of 1 for any volume element (voxel) with gray-scale value greater than the threshold. The head volume was separated from noise and motion artifacts occupying the space surrounding the head by applying first applying an OPEN image processing operator (an ERODE operator followed by a DILATE operator); for each of these steps, 3x3x3 cubic shape element was used as the convolution kernel. The resulting mask image was multiplied by a 20x20x20 cubic element located at the image center to generate a seed volume. The seed volume was input into a region-growing algorithm that used successive steps of convolving the mask image with a cubic kernel. The result was a mask image containing only the connected head volume. For subsequent calculations, a unit density was assumed for each non-zero voxel in the mask.

Head Center-of-Mass Calculation: The center-of-mass (COM) of the binarized mask image was computed by first summing, over all non-zero voxels, the distance between each voxel the origin; this sum divided by the total number non-zero voxel count yielded the COM.

Inertia Tensor Analysis: The inertia tensor **I** of a rigid object is determined by the mass distribution

within the object. It is a 3x3 matrix that characterizes the angular momentum of a rigid object when spun about a reference point with given angular velocity. For the head mask image, the inertia tensor with respect to the COM was calculated according to the following equations, assuming a mass density of one.

$$I_{(0,0)} = \sum \; y_i^2 + z_i^2$$
$$I_{(1,1)} = \sum \; x_i^2 + z_i^2$$
$$I_{(2,2)} = \sum \; x_i^2 + y_i^2$$
$$I_{(0,1)} = I_{(1,0)} = \sum \; x_i y_i$$
$$I_{(1,2)} = I_{(2,1)} = \sum \; y_i z_i$$
$$I_{(0,2)} = I_{(2,0)} = \sum \; x_i z_i$$

Where x, y and z are the component distances of each non-zero voxel from the center-of-mass, i is the voxel index and $\sum$ denotes the summation over i. The three principal axes of the inertia tensor were found using eigen-analysis to solve for the eigenvalues (magnitudes of the principal moments of inertia) and eigenvectors (directions of the principal axes) of the inertia tensor.

To predict whether the true orientation of the head matched the orientation recorded in the image header, a calculation was made of the vector product between each subject's principal axis vector and the sample group median principal axis vector. The same vector product was computed again after transforming the sample group median principal axis vector to a new orientation corresponding to the two test cases of possible orientation labeling errors described in the section below.

Boundary Mid-Point Calculation: After alignment of the brain along the 3 principal inertial axes, the boundaries of the head with respect to each axis plane were determined. The positions of the non-zero voxels furthest to the left, right, etc. of the COM for each direction were computed, and the midpoint between these boundaries was termed the boundary mid-point (BMP). The difference between the COM and BMP was calculated for each brain and group differences in the sign and magnitude of this shift were tested to determine whether they could detect errors in orientation labeling.

Orientation Mislabeling Test Cases: The above computations were performed for the default case of proper orientation labeling and for each of two cases of erroneous labeling that would result in swapping of right and left on the images:

1) labeled orientation: Supine Head First, actual orientation: Prone Head First
2) labeled orientation: Supine Feet First, actual orientation: Supine Head First

Other orientation labeling errors are possible, but the difference measured by our technique would equal that of one of the cases above, therefore only the above cases need to be tested to evaluate the methodology.

Results

For all subjects in the sample group, the direction of the inertial principal axis corresponding to the smallest eigenvalue (the axis with highest symmetry) was directed in the general direction of the anterior-posterior axis of the brain and was aligned approximately parallel with a line connecting the anterior cingulate and posterior cingulate. Figures 1 and 2 show the X, Y and Z components of the principal axis for the sample and test groups.
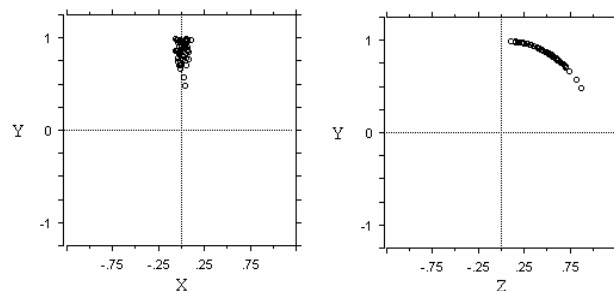

Figure 1. The inertia tensor principal symmetry axis is plotted on the x-y plane (left) and the y-z plane (right) for the sample group of 56 normal subjects that was used to generate the prediction model equations. x, y and z are the left-right, anterior-posterior & superior-inferior directions, respectively.
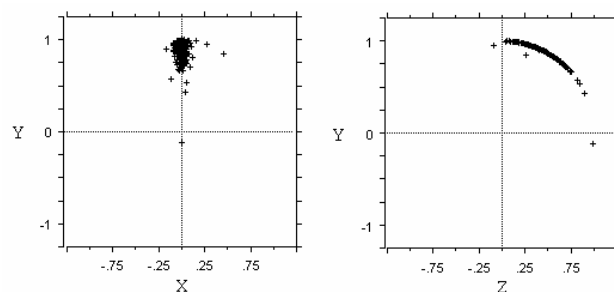

Figure 2. The inertia tensor principal symmetry axis is plotted for the test group composed of 57 normal subjects and 89 patients with brain pathology.

A single brain had a negative principal axis Y component, due to a field-of-view wrap-around artifact, which caused the inferior portion of the neck to appear on the superior edge of the image. For this individual, the vector product provided an incorrect prediction of head orientation. For the one case where the shift between COM and BMP was opposite in sign from all others, the inertia analysis gave the correct prediction when the COM-BMP shift had predicted incorrectly. The inertial principal axes cannot be differentiated from their polar negatives. The sign of the Y component of the COM-BMP shift must be used to determine the polarity of the Y principal component axis. Therefore, in the single case with negative COM-BMP Y component, a false prediction was made that the orientation was not head first supine.

Figure 3 shows the Y (anterior-posterior) and Z (superior-inferior) components of the distance between COM and BMP for the sample and test groups. In the sample group, COM was shifted in all subjects in the superior and posterior directions by a mean of 7.1 mm and 7.5 mm, respectively, reflecting the top-heavy and posterior-heavy shape of the human head. In the test group, only 1 schizophrenic subject had an inverted Y shift. This was caused by large motion artifacts resulting from motion in the throat, probably swallowing, and movement of the eyes.
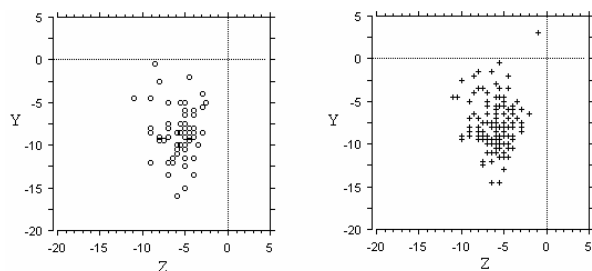

Figure 3. The y and z components of the distance between the center-of-mass (COM) and the boundary mid-point (BMP) is plotted for the sample group (left) and test group (right). One subject had a positive shift in the y direction, which resulted in a false prediction of orientation mislabeling.

For 50 subjects, their images were flipped in the anterior-posterior or superior-inferior directions and the analysis run to predict proper orientation. In every case, the mismatch between the assumed orientation (supine head first) and the altered orientation was detected.

No false negative predictions were made, therefore the measured sensitivity of the method was 100%. The specificity was 98% due to 2 false positives.

Discussion

Images that reside on digital image record systems are considered reliable, since this is generally true. Mislabeling errors that become incorporated in such systems can lead directly to misdiagnoses and treatment errors involving laterality such as wrong-side surgery or wrong side radiation treatment.

Conclusion

The orientation-testing algorithm presented here had high sensitivity and specificity for mislabeling errors, suggesting it could prove useful for detecting such errors in a clinical setting. It is entirely automated, easily implemented and fast enough to run on any computer workstation that is integrated into an MRI or CT scanner or other digital imaging device. A prediction of probable mislabeling would produce a warning message prompting the imaging device operator to check for a mismatch between the orientation selected in software and the actual patient orientation. This would enable the correction of errors at the time and place they first occur and before they are incorporated into the radiology image record system.

References

1) Steinhauer J. So, the tumor is on the left, right?; Seeking ways to reduce operating room errors. New York Times. April 21, 2001.
2) Beyea SC. Ensuring correct site surgery. AORN Journal. 2002; 76(5): 880-882.
3) Berstein M. Wrong-side surgery: systems for prevention. Can. J. Surgery. 2003; 46(2): 144-146.
4) JCAHO. Universal Protocol for Preventing Wrong Site, Wrong Procedure, Wrong Person Surgery. 2003. ww.jointcommission .org /PatientSafety/UniversalProtocol.
5) AAOS Advisory Statement on Wrong Site Surgery, September 1997.
6) Oregon Assoc. of Hospitals and Health Care Systems. Hints on preventing surgery on the wrong site. www.aracnet.com/ ~oahhs/issues/safety/surgery.htm.

7) The Institute for Healthcare Improvement (www.ihi.org).

8) Schmidt D and Odland R. Mirror-image reversal of coronal computed tomography scans. The Laryngoscope. 2004; 114: 1562-1565.

9) Christensen JD, Wang Y, Mosier KM, Kalnin AJ, Kronenberger WG, Dunn DW & Matthews VP. Abnormal Inter-hemispheric Brain Asymmetry in Adolescents with Disruptive Behavioral Disorder. Proceedings Intl. Soc. Magn. Reson. Med. Annual Meeting, 2006.